Holger Dorrer*, Katerina Chrysalidis, Thomas Day Goodacre, Christoph E. Düllmann, Klaus Eberhardt, Christian Enss, Loredana Gastaldo, Raphael Haas, Jonathan Harding, Clemens Hassel, Karl Johnston, Tom Kieck, Ulli Köster, Bruce Marsh, Christoph Mokry, Sebastian Rothe, Jörg Runke, Fabian Schneider, Thierry Stora, Andreas Türler and Klaus Wendt

Production, isolation and characterization of radiochemically pure ^{163}Ho samples for the ECHo-project

https://doi.org/10.1515/ract-2017-2877
Received September 7, 2017; accepted January 17, 2018; published online March 6, 2018

Abstract: Several experiments on the study of the electron neutrino mass are based on high-statistics measurements of the energy spectrum following electron capture of the radionuclide ^{163}Ho. They rely on the availability of large, radiochemically pure samples of ^{163}Ho. Here, we describe the production, separation, characterization, and sample production within the Electron Capture in Holmium-163 (ECHo) project. ^{163}Ho has been produced by thermal neutron activation of enriched, prepurified ^{162}Er targets in the high flux reactor of the Institut Laue-Langevin, Grenoble, France, in irradiations lasting up to 54 days. Irradiated targets were chemically processed by means of extraction chromatography, which allowed separating the formed Ho from the ^{162}Er target-material and from the main byproducts ^{170}Tm and ^{171}Tm, which are co-produced in GBq amounts. Decontamination factors of >500 for Er and of $>10^5$ for Tm and yields of $3.6 \cdot 10^{16}$ and $1.2 \cdot 10^{18}$ atoms of ^{163}Ho were obtained, corresponding to a recovery yield of 95 % of Ho in the chemical separation. The Ho-fraction was characterized by means of γ-ray spectrometry, Inductively-Coupled-Plasma Mass Spectrometry (ICP-MS), Resonance Ionization Mass Spectrometry (RIMS) and Neutron Activation Analysis (NAA). In this process, the thermal neutron capture cross section of ^{163}Ho was measured to $\sigma_{\text{Ho-163 to Ho-164m}} = (23 \pm 3)$ b and $\sigma_{\text{Ho-163 to Ho-164g}} = (156 \pm 9)$ b for the formation of the two isomers of ^{164}Ho. Specific samples were produced for further purification by mass separation to isolate ^{163}Ho from the Ho-isotope mixture, as needed for obtaining the energy spectrum within ECHo. The partial efficiency for this second separation step is (32 ± 5) %.

Keywords: Neutrino mass determination, ^{163}Ho, neutron activation, lanthanide separation, extraction chromatography.

***Corresponding author: Holger Dorrer,** Johannes Gutenberg-Universität Mainz, Mainz, Germany; Universität Bern, Bern, Switzerland; and Paul Scherrer Institut, Villigen, Switzerland, E-mail: Holger.Dorrer@uni-mainz.de; Holger.Dorrer@web.de
Katerina Chrysalidis, Klaus Eberhardt, Raphael Haas, Tom Kieck, Christoph Mokry, Fabian Schneider and Klaus Wendt: Johannes Gutenberg-Universität Mainz, Mainz, Germany
Thomas Day Goodacre and Sebastian Rothe: CERN, Geneva, Switzerland; and University of Manchester, Manchester, UK
Christoph E. Düllmann: Johannes Gutenberg-Universität Mainz, Mainz, Germany; and GSI Helmholtzzentrum für Schwerionenforschung, Darmstadt, Germany
Christian Enss, Loredana Gastaldo and Clemens Hassel: Universität Heidelberg, Heidelberg, Germany
Jonathan Harding: Johannes Gutenberg-Universität Mainz, Mainz, Germany; and Cardiff University, Cardiff, UK
Karl Johnston, Bruce Marsh and Thierry Stora: CERN, Geneva, Switzerland
Ulli Köster: Institut Laue-Langevin, Grenoble, France
Jörg Runke: GSI Helmholtzzentrum für Schwerionenforschung, Darmstadt, Germany
Andreas Türler: Universität Bern, Bern, Switzerland; and Paul Scherrer Institut, Villigen, Switzerland

1 Introduction

The determination of the neutrino masses is one of the major challenges of contemporary particle physics. Different approaches are followed to push the boundaries of achievable sensitivity. Among them, experiments exploring the beta decay and electron capture processes of suitable nuclides promise to provide model-independent information on the electron (anti)-neutrino mass value. The electron capture in holmium-163 experiment, ECHo [1–3], is designed to investigate the electron neutrino mass in the sub-eV/c^2 range. This can be achieved by the analysis of the calorimetrically measured energy spectrum following the electron capture (EC) process of ^{163}Ho. This is an artificial radionuclide with a half-life $T_{1/2}$ of (4570 ± 50) a [4]. It decays by EC with a very low Q-value to

the ground-state of ^{163}Dy. Production of ^{163}Ho is achieved via different pathways. More specifically, these include reactor production by irradiating enriched ^{162}Er targets, or accelerator production using light-particle induced reactions on suitable targets. Different collaborations aiming to develop sensitive experiments based on ^{163}Ho have chosen different production pathways [5]. Besides the need for separating Ho from a wealth of neighboring elements, including the target material, a specific aspect of all these experiments is the separation of ^{163}Ho from long-lived ^{166m}Ho ($T_{1/2} = 1200$ a [6], β^-/γ-emitter), the presence of which severely disturbs the electron neutrino mass determination. The different production pathways feature different intrinsic ^{163}Ho/^{166m}Ho ratios. According to the results obtained in [7], an accelerator-based production pathway appears more favorable in this respect. Reactor-based approaches, however, benefit from larger projectile fluxes and cross sections as well as the often better availability of reactor irradiation time. The ECHo collaboration has thus focused on this pathway so far, while evaluation of the accelerator pathway is continued in more detail [1, 8] in parallel. After production, high-performance chemical separation of the ^{163}Ho from the target material is required. Interesting processes have been already developed in the case of accelerator production using Dy targets [9]. Recent work on the separation of Ho from Er has been performed in the context of a re-measurement of the ^{166m}Ho half-life [10]. Separation of ^{166g}Ho from reactor-irradiated Dy targets is described in [11, 12].

Here, we present the production of milligram amounts of ^{163}Ho via neutron-irradiation of Er samples enriched in ^{162}Er in the high-flux reactor at the Institut Laue-Langevin (ILL), Grenoble, France, and the development of a high-performance chemical separation procedure for the produced ^{163}Ho from the massive Er targets as well as co-produced contaminants (most importantly GBq amounts of ^{170,171}Tm).

The energy spectrum following EC decay in ^{163}Ho will be measured by embedding the ^{163}Ho in metallic magnetic calorimeters (MMCs) [13], which exhibit optimum performance for the task at hand. The preparation of the required, isotopically pure samples by mass separation of the Ho samples and the implantation into the MMCs is described in [14]. Separate samples have been prepared for high-precision measurements of the Q_{EC} value of ^{163}Ho using Penning-Trap Mass Spectrometry (PTMS) [15] to provide a value independent of that evaluated from the energy spectrum, and the corresponding measurement of the Q_{EC} value was recently performed [16].

2 Experimental

2.1 Prepurification of erbium target material and neutron irradiation

Neutron activation of stable nuclides generally induces (n,γ) nuclear reactions, which lead to a more neutron-rich isotope of the same element. In many cases, this isotope is radioactive and undergoes β^--decay to the isobaric nuclide of the next heavier element. Notable exceptions occur for neutron-deficient nuclides like ^{162}Er or ^{164}Er, whose (n,γ) products are still neutron-deficient and thus undergo β^+/EC-decay to the isobaric nuclide of the adjacent lighter element, i.e. Ho in the case of Er.

Lower-Z ($Z < 68$) nuclides are otherwise most dominantly produced only in rather unimportant side-reactions occurring with small probability, involving charged-particle emission following neutron-irradiation. In contrast, higher-Z nuclides are abundantly produced as byproducts during neutron irradiation. Overall, this results in the fact that most impurities lead to nuclides with higher Z, while the target isotope ^{162}Er yields the lower-Z product ^{163}Ho. In this context it is noteworthy to mention that commercially available Er samples typically contain trace amounts of impurities, including other lanthanides. Therefore, our strategy for the production of radiochemically pure Ho samples includes the removal of elements with Z below that of Er prior to irradiation, during which these would lead to the production of further undesired byproducts. At the same time, such a prepurification also minimizes the formation of ^{166m}Ho by reduction of the trace amounts of ^{164}Dy and ^{165}Ho present in the commercially available enriched ^{162}Er. Removal of above-target lanthanide impurities prior to irradiation is less critical as many above-target radionuclides will be produced from the Er target, and further because the elements above Ho will be removed anyway after irradiation along with the Er target element. In the same way, the elimination of impurities of strongly-activating elements as Sc, Co, Eu, Ta, and Ir, leading to neutron-capture products having rather long half-lives is additionally very important to minimize the dose rate of the irradiated sample.

Figure 1 shows the main steps involved in the production and chemical isolation procedure for ^{163}Ho. An initial amount of 46 mg Er in the chemical form of $\{^{162}Er\}Er_2O_3$ (Oak Ridge National Laboratory, Tennessee, USA) with the Er isotope distribution of (20.4 ± 0.1) % ^{162}Er, (3.91 ± 0.05) % ^{164}Er, (33.5 ± 0.1) % ^{166}Er, (17.6 ± 0.1) % ^{167}Er, (17.3 ± 0.1) % ^{168}Er, and (7.29 ± 0.1) % ^{170}Er was dissolved in concentrated nitric acid (65 %, Suprapur, VWR, Darmstadt, Germany).

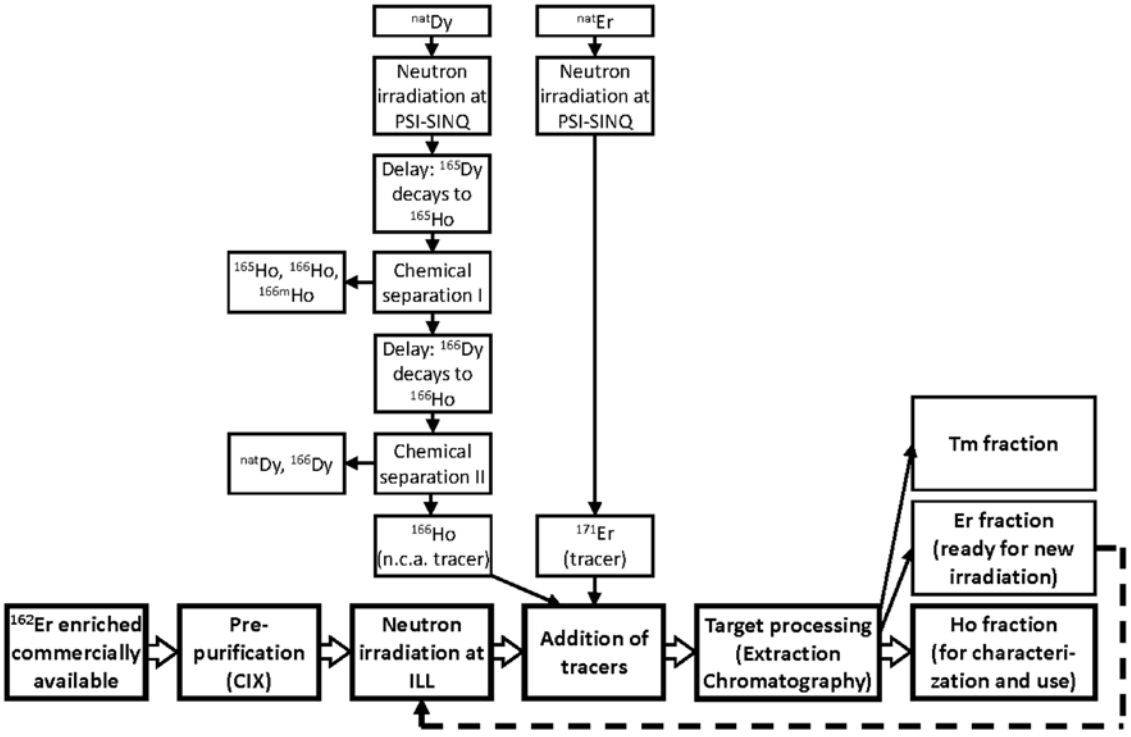

Figure 1: Block diagram showing the production and isolation strategy of ^{163}Ho.

After evaporation to dryness the residue was redissolved in MilliQ-water (18.2 MΩ · cm, Millipore water purification system, Milli-Q-Biocel, Millipore AG, Zug, Switzerland) and loaded onto a 9 mm diameter · 300 mm length cation exchange column (GE Healthcare Europe GmbH, Glattbrugg, Switzerland), filled with a strongly acidic, macroporous cation exchange resin in its NH_4^+-form. Elution was performed with 0.1 M α-hydroxy isobutyric acid (α-HIBA, Sigma Aldrich, Steinheim, Germany) solution, adjusted with concentrated ammonia (25 %, Suprapur, VWR, Darmstadt, Germany) to pH = 5 prior to use. The eluate was collected in 10 mL fractions. Relevant fractions for Er, which were identified in a prior test separation of neutron-activated Er (natural isotopic composition) via the 308-keV γ line of ^{171}Er (analyzed by γ-ray spectrometry using a high purity germanium detector EURISYS Mesures, EGC 06-185-R operated with Interwinner 5.0 software, Baechli instruments, Affoltern am Albis, Switzerland), as well as the unpurified starting material were analyzed by inductively-coupled plasma optical emission spectroscopy (ICP-OES) for Sc, Co, Eu, Gd, Tb, Dy, Ho, Ta, and Ir. Their presence would result in relatively long-lived radioactive byproducts produced with high yields in neutron irradiations. The purified Er fractions were acidified with concentrated nitric acid (65 %, Suprapur) and loaded onto a cation exchange column (5 mm diameter · 180 mm length, H^+-form). The column was rinsed with MilliQ-water and 1 M nitric acid. Afterwards the Er was stripped with 4 M nitric acid. The obtained Er solution was evaporated to dryness and redissolved in MilliQ-water. Two irradiation targets of 6.7 mg and 30 mg Er were prepared by evaporation of aliquots of this solution in quartz ampoules (suprasil, Heraeus, Kleinostheim, Germany), which were subsequently sealed for irradiation.

The quartz ampoules were irradiated in the high flux reactor of Institut Laue-Langevin (Grenoble, France) at (unperturbed) thermal neutron fluxes of $\approx 1.4 \cdot 10^{15}$ cm$^{-2} \cdot$ s^{-1} (6.7 mg target) for 3.9 days and $\approx 1.3 \cdot 10^{15}$ cm$^{-2} \cdot$ s^{-1} (30 mg target) for 53.7 days.

2.2 Isolation of holmium from the irradiated erbium targets

2.2.1 Production of tracers ^{166}Ho and ^{171}Er

Tracers of ^{166}Ho (without ^{166m}Ho) and ^{171}Er were produced by neutron activation of 10 mg ^{nat}Dy und 1 mg ^{nat}Er at the spallation neutron source SINQ of Paul Scherrer Institut (Villigen, Switzerland) (cf. Figure 1). No carrier added (n.c.a.) ^{166}Ho was isolated from the irradiated ^{nat}Dy target in a two step separation procedure: the target was dissolved in 0.1 M nitric acid and afterwards loaded onto an extraction chromatographic column (10 mm diameter, ca. 250 mm length),

filled with LN resin (Triskem, Bruz, France). The elution of the column was performed with 1 M nitric acid applying a flow rate of 0.5 mL/min and the eluate was collected in 10 mL fractions, which were analyzed by γ-ray spectrometry for their ^{166}Dy and ^{166}Ho content. Dy containing fractions were unified, evaporated to dryness and redissolved in 0.1 M nitric acid. The process was repeated in the same way for the isolation of ^{166}Ho formed in the decay of ^{166}Dy.

The Er-tracer obtained from the activated ^{nat}Er was dissolved in 0.1 M nitric acid after its production.

2.2.2 Chemical isolation of Ho

The irradiated ^{162}Er targets were processed following a 4-months cooling period after irradiation. The quartz ampoules containing the neutron irradiated ^{162}Er were crushed and their content was dissolved in 0.1 M nitric acid. The tracers of n.c.a. ^{166}Ho and ^{171}Er were added (cf. Figure 1) to enable the monitoring of the distribution of Ho and Er in the later separation process by γ-ray spectrometry. The mixture was loaded onto the same chromatographic column, which has been used for the previously described Ho-tracer isolation. The elution of the column and the collection of the fractions was done in an analogous way as the separation of the ^{nat}Dy target, but applying 2 M instead of 1 M nitric acid. The fractions were analyzed by γ-ray spectrometry (using the above mentioned detector) for their ^{166}Ho, ^{171}Er, and ^{170}Tm activities.

Exclusively the Ho containing fractions isolated from the same target were unified and evaporated to dryness. The residue after evaporation was surveyed for radioactive impurities by γ-ray spectrometry using the germanium detector system specified in Section 2.1, and afterwards dissolved in 1 mL (Ho isolated from 6.7 mg Er-target) or 5 mL (Ho from 30 mg Er-target) MilliQ-water. Small aliquots of these samples were employed for the Penning-trap mass measurements of ^{163}Ho as reported in [15, 16].

The Er fractions were unified separately and are available as starting material for a new neutron irradiation at ILL for ^{163}Ho production (cf. Figure 1).

2.3 Characterization of the isolated holmium samples

To perform a more detailed analysis of the obtained Ho samples, including the determination of the stable isotopes content (especially Ho and Dy), further analytical techniques have been applied.

For Inductively-Coupled-Plasma Mass Spectrometry (ICP-MS) analysis aliquots of 100 µL solution of Ho isolated from the 6.7 mg Er-target or 5 µL solution of Ho isolated from the 30 mg Er-target were added to 900 µL and 995 µL MilliQ-water, respectively. These samples were further diluted by 4 % nitric acid by factors of 1000 and 8196, respectively. Ir was added as internal standard to 100 ppb concentration in the solutions. The measurement was performed using an ICP-MS 7500ce (Agilent Technologies, Santa Clara, USA). The absolute concentrations of ^{165}Ho (calibration curve done with stable Ho) as well as the isobar ratios from 157 u to 174 u and 193 u (Ir standard) were determined. Additionally, a sample of the 4 % nitric acid used for dilution was analyzed in the same way as background measurement. The results were corrected by subtraction of this background.

Resonant Ionization Mass Spectrometry (RIMS) was applied for analysis of the isotope ratios of Dy in both samples. The RISIKO mass separator at the Institut für Physik, Johannes Gutenberg-Universität Mainz [14, 17] was employed. Aliquots also of 10 µL were evaporated to dryness on Zr foil pieces (Alfa Aesar, Karlsruhe, Germany, 5 mm · 5 mm large, 0.025 mm thickness). Some metallic Y (more than 10 times the amount of the sample) was sputtered from a massive Y foil (Goodfellow, Bad Nauheim, Germany, 25 mm · 25 mm large, 0.125 mm thickness, 99 % purity with respect to the content of the remaining rare earth elements) over the evaporated sample aliquots on the Zr foils by use of pulsed laser deposition in an external vacuum chamber. After finishing the sputtering procedure the samples sputtered with Y were immediately transferred into the RISIKO ion source after venting the vacuum chamber with argon in order to minimize the contact of the Y metal with the ambient air. The tantalum ion source of the RISIKO facility was resistively heated by a current of about 170 A to a temperature in the range of 1300–1600 K. Ionization specific to the single element Dy was accomplished by the use of a dedicated resonant three stage laser excitation scheme based on laser radiation of 404.71 nm, 802.72 nm, and 837.66 nm wavelength [18]. Obtained ions were extracted from the ion source by applying a high voltage of 30 kV, followed by mass separation in a homogenous electromagnetic 60° sector field of 0.43 T. The detection of the ions is achieved by a Faraday cup where secondary electrons are suppressed by a repeller electrode and measurement of the resulting current by a picoamperemeter (Keithley 617, Tektronix UK Ltd., Berkshire, UK). Mass spectra were recorded by varying the field strength of the magnet in the range corresponding to collect ions of masses from 159 u to 167 u in the focal plane. After normalization to the temporal evolution of the total ion beam intensity, the Dy isotopic composition was determined this way. Additionally a background measurement of a blank

Zr foil sputtered with an equal amount of Y without any sample had been performed in order to check the potential introduction of Dy-isotopes from these materials. As given in Section 3.3, no stable Dy-ion beam resulted.

Neutron activation analysis (NAA) was applied to determine the absolute content of ^{164}Dy. For this, aliquots also of 10 µL of the solutions described at the end of Section 2.2 were evaporated to dryness in small polyethylene (PE)-capsules and then irradiated in the carousel irradiation position of the TRIGA Mainz research reactor at a thermal neutron flux of about $7 \cdot 10^{11}$ cm$^{-2} \cdot$ s^{-1} for 60 min. Simultaneously, two 3.2 mg and 4.0 mg pieces of Al-Au wire (Ortec GmbH, Munich, Germany) containing 0.1124 % Au were irradiated in separate PE-capsules placed at the bottom and top of the two stacked sample capsules for neutron flux determination. Subsequently, the aliquots of both solutions and the Al-Au wire pieces were measured repeatedly by γ-ray spectrometry using a high purity germanium detector (Canberra GX7020, relative efficiency ≥70 %) in the range of 15 min to 3 days after the end of irradiation.

2.4 Magnetic isotope separation for isolation of ^{163}Ho from chemically purified Ho fractions

The ^{163}Ho samples obtained after the chemical separation described in Section 2.2 contain minor amounts of ^{166m}Ho as the sole radioactive contaminant of concern for ECHo. For its removal, magnetic isotope separation is applied, which is suitable to suppress this contaminant sufficiently well. Therefore, samples obtained after the procedure described in Section 2.2 were used as source for subsequent laser resonance ionization and magnetic isotope separation [19]. Besides the primary purpose of removal of ^{166m}Ho, this step also enabled a reduction of the ^{165}Ho content (important to avoid significant changes in heat capacity of the MMCs). As one of the main applications of radiochemically pure ^{163}Ho for ECHo involves the preparation of samples fully embedded in the MMCs, the mass separation step simultaneously enabled the direct implantation of the ^{163}Ho ions into the ECHo MMCs [14]. The RISIKO and the General Purpose Separator (GPS) at CERN-ISOLDE [20] were tested and applied for this process of separation and implantation. Samples of the mixture of ^{163}Ho, ^{165}Ho and ^{166m}Ho were prepared on Ti foil pieces (Alfa Aesar, Karlsruhe, Germany, 5 mm · 5 mm large, 0.0127 mm thickness for mass separation at RISIKO; Goodfellow, Bad Nauheim, Germany, 10 mm · 10 mm large, 0.0125 mm thickness for use at ISOLDE) in the procedure as follows: A hemispherically-shaped depression was pressed into the center of the foils and it was afterwards filled with 1–20 µL of solution, which is described at the end of Section 2.2, followed by evaporation at 80 °C. Accordingly, samples with a ^{163}Ho content in the order of 10^{14} to 10^{16} atoms were inserted into ovens connected to the ion sources of the mass separators. Additionally, ^{nat}Ho samples containing a known amount of ^{165}Ho (either 10^{14} or 10^{15} atoms) were prepared for measurements of the ionization- and transmission-efficiency of RISIKO for Ho [14].

For separation using the GPS, the ^{163}Ho was ionized by the ISOLDE RILIS [21] using an ionization scheme specifically investigated for this experiment. A three-step RILIS ionization scheme of (λ_1, λ_2, λ_3) = [406 nm, 623 nm, 532 nm (not resonant)] [22] was applied, resulting in an enhancement factor of 55 compared to surface ionization alone. Details of the optimization and adaptation of the RISIKO mass separator regarding the laser ionization process, the ion source lay-out and a final post-focalization stage will be given elsewhere.

3 Results and discussion

3.1 Prepurification of the erbium target and irradiation

According to the results of the ICP-OES analysis, the initial 46 mg of ^{162}Er-enriched Er contained 0.83 µg of Eu, 82 µg of Dy, and less than 11 µg of Ho, whereas contents of all other elements analyzed for were below the limit of quantification. Chemical purification of this portion of enriched ^{162}Er material by cation exchange chromatography resulted in the 10 mL fractions given in Table 1. Fractions 6 to 13 were

Table 1: Results of ICP-OES measurement of relevant fractions of ^{162}Er-enriched Er after chemical separation.

Fraction no.	Elution-time	Dy (µg)	Ho (µg)	Er (µg)
6	50–60 min	–	–	2105
7	60–70 min	–	–	3794
8	70–80 min	–	–	7252
9	80–90 min	–	–	8793
10	90–100 min	–	2	9777
11	100–110 min	3	2	10,422
12	110–120 min	92	–	1397
13	120–130 min	–	–	2
Q. L.[a]	–	0.5	2	0.5

Fractions 6–11 were used for the neutron-irradiation at ILL Grenoble.
[a]Q. L., Quantification limit. Values below the quantification limits were obtained for Sc (0.5 µg), Co (10 µg), Eu (0.2 µg), Gd (2 µg), Tb (2 µg), Ta (2 µg), Ir (3 µg).

analyzed for all the chemical elements mentioned in the footnote of Table 1; fractions 6 to 11 were used for the erbium targets. The separation provided thus a total yield of 92 %.

About 97 % of the Dy contained in the Er as obtained from the supplier were removed by the purification procedure. Concerning the Ho content, no strict quantitative statements are possible as the content is close to the quantification limit; furthermore, the distribution follows that of Er, which might reflect some interference of the at least 4000-fold higher Er concentration.

During irradiation of the Er with thermal neutrons ^{163}Er, decaying by EC with a half-life of 75 min to ^{163}Ho, is formed by neutron capture of ^{162}Er. The number of ^{163}Ho atoms $N_{^{163}Ho}$ produced within an irradiation of the duration t_I can be calculated using eq. 1.

$$N_{^{163}Ho} = N_{^{162}Er_0} \cdot \sigma_{^{162}Er} \cdot \phi \cdot \lambda_{^{163}Er} \cdot \frac{\left[\left(\lambda_{^{163}Er} + \sigma_{^{163}Er}\cdot\phi - \left(\sigma_{^{162}Er}\cdot\phi + \sigma_{^{163}Ho}\cdot\phi\right)\right)\cdot e^{-\sigma_{^{162}Er}\cdot\phi\cdot t_I} + \left(\lambda_{^{163}Ho} + \sigma_{^{163}Ho}\cdot\phi - \sigma_{^{162}Er}\cdot\phi\right)\cdot e^{-\left(\lambda_{^{163}Er}+\sigma_{^{163}Er}\cdot\phi\right)\cdot t_I} \ldots \right.}{\left[\left(\lambda_{^{163}Er} + \sigma_{^{163}Er}\cdot\phi - \sigma_{^{162}Er}\cdot\phi\right)\cdot\left(\lambda_{^{163}Er} + \sigma_{^{162}Er}\cdot\phi - \left(\lambda_{^{163}Ho} + \sigma_{^{163}Ho}\cdot\phi\right)\right)\ldots\right.}$$
$$\left. \frac{-\left(\lambda_{^{163}Er} + \sigma_{^{163}Er}\cdot\phi - \sigma_{^{162}Er}\cdot\phi\right)\cdot e^{-\left(\lambda_{^{163}Ho}+\sigma_{^{163}Ho}\cdot\phi\right)\cdot t_I}}{\left(\lambda_{^{163}Ho} + \sigma_{^{163}Ho}\cdot\phi - \sigma_{^{162}Er}\cdot\phi\right)}\right] \quad (1)$$

where $N_{^{162}Er_0}$ is the number of ^{162}Er atoms at the start of the irradiation, ϕ the thermal neutron flux, λ_i the decay constant of isotope i, σ_i the thermal neutron capture cross section of isotope i, and t_I the duration of the neutron irradiation.

There are no reliable data available for the neutron capture cross sections of ^{163}Er and ^{163}Ho. Thus, values of 0 barn were used for initial estimates of the ^{163}Ho content after irradiation. This approach corresponds to neglecting the double-neutron capture to ^{164}Er as well as the product burn-up of ^{163}Ho. In an analogous way, the production of ^{165}Ho from the neutron capture on ^{164}Er, the latter being present with an isotopic abundance of (3.91 ± 0.05) % in the Er targets, can be estimated with results as given in Table 2. Note that these values tend to be overestimated since they are based on the "unperturbed" neutron flux. Self-attenuation by the sample and its encapsulation will reduce the effective ("perturbed") flux. Initially the self-attenuation in the target is dominated by the ^{167}Er content that is, however, reduced over time through burnup.

These results show that the amount of stable Ho formed during the irradiation due to neutron capture on ^{164}Er exceeds the amount of Ho, which may have been present after chemical separation due to incomplete Ho removal.

Table 2: Calculated ^{163}Ho and ^{165}Ho content (atom numbers) after irradiation.

Nuclide	6.7 mg Er target (atoms)	30 mg Er target (atoms)
^{163}Ho (from ^{162}Er)	$4.4 \cdot 10^{16}$	$2.5 \cdot 10^{18}$
^{165}Ho (from ^{164}Er)	$5.7 \cdot 10^{15}$	$2.8 \cdot 10^{17}$
^{165}Ho (initially present)[a]	$6.9 \cdot 10^{15}$ (1.9 μg)	$3.1 \cdot 10^{16}$ (8.5 μg)

[a]Assuming no loss of Ho in chemical prepurification, cf. Section 3.1.

3.2 Isolation of holmium from the irradiated targets

After the cooling period of four months, the activity of the irradiated Er-targets was dominated by up to GBq amounts of the relatively long-lived side-products ^{170}Tm ($T_{1/2}$ = 128.6 days) and ^{171}Tm ($T_{1/2}$ = 1.92 a), which were produced from ^{167}Er [(17.6 ± 0.1) % isotopic abundance in the target], ^{168}Er [(17.3 ± 0.1) %] and ^{170}Er [(7.29 ± 0.05) %]. Initial γ-ray spectrometric analysis of the irradiated ampoules prior to further processing resulted in values of 3.6 MBq ^{170}Tm and 35.5 MBq ^{171}Tm for the 6.7 mg target and 3.3 GBq ^{170}Tm and 2.5 GBq ^{171}Tm for the 30 mg target at the end of bombardment (EOB). These unwanted Tm byproducts as well as the excess of remaining Er needed to be separated from the produced Ho.

Short-lived, γ-emitting radioisotopes of Ho and Er were added to enable the monitoring of the Ho and Er distribution by γ-ray spectrometry during chemical separation. Suitable tracers are ^{166}Ho ($T_{1/2}$ = 26.80 h) and ^{171}Er ($T_{1/2}$ = 7.52 h), since they have suitable γ lines and are short-lived enough for their complete decay after the separation, before the further use of Ho [for Electromagnetic Mass (EM) separation and implantation] and Er (for a new neutron irradiation cycle). ^{166}Ho was used in n.c.a. quality to avoid introduction of additional ^{165}Ho and ^{166m}Ho, as would happen with neutron activated ^{165}Ho tracer. As shown in Figure 1, the ^{166}Ho had been prepared from a neutron irradiated ^{nat}Dy target in two separation steps and added to the solution of the irradiated targets prior to the Ho isolation (cf. Figure 1). About 250 kBq of ^{166}Ho and

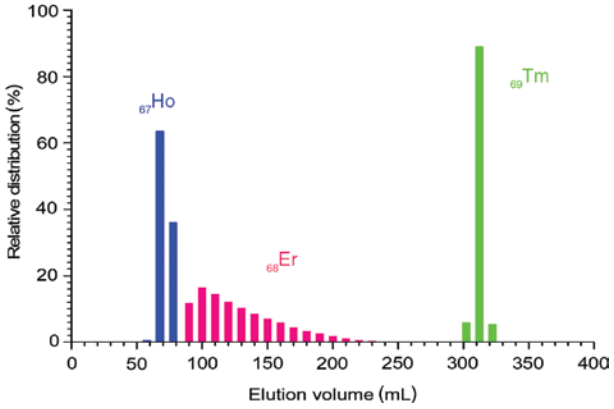

Figure 2: Elution profile of the 30 mg Er-target separation, performed by extraction chromatography at room temperature applying a flow rate of ~0.5 mL/min of eluate.
The separation was monitored by tracing ^{166}Ho, ^{171}Er, and ^{170}Tm with γ-ray spectrometry. No Er above detection limit was found in the last Ho-containing fraction, and no Ho above detection limit in the first Er-containing fraction.

400 kBq ^{171}Er were added to each of the irradiated targets before the chemical separation.

Figure 2 shows the elution profile of the column chromatographic separation of the 30 mg Er-target, which evidences successful separation of the three adjacent lanthanides Ho, Er and Tm. The desired Ho was obtained within 30 mL of the eluate (from 50 mL to 80 mL elution volume). A Ho recovery yield of 95.4 % was achieved for the 30 mg Er-target. The last Ho fraction was directly followed by the first Er fraction. No Er-activity was detected in the Ho fraction and no Ho-activity in the Er-fractions. A more detailed analysis (see Section 3.3) quantified the remaining amount of Er (from all stable Er isotopes) in the Ho fraction after its isolation from the irradiated target to about one eighth of the produced ^{163}Ho, whereas ^{169,170,171}Tm were present in amounts lower than our detection limit. The decontamination factors achieved in the separation were experimentally determined to 560 ± 70 for Er and $>2.3 \cdot 10^5$ for Tm (based on the evaluation of ^{170}Tm). Isolation of Ho from the 6.7 mg Er-target was performed in the same way, and a recovery of 99.4 % was achieved. In contrast to the separation of the 30 mg Er-target, no remaining Er was found, not even via a more detailed analysis (see Section 3.3) of the Ho sample.

3.3 Characterization of the isolated holmium samples

The ^{163}Ho does not emit any γ radiation, in contrast to the relevant irradiation byproducts, which have easily detectable γ lines of sufficient intensity. Analysis via γ-ray spectrometry is therefore an excellent method for obtaining information about the presence of such γ-ray emitting byproducts in the produced ^{163}Ho. In the ideal case of ^{163}Ho being the sole radionuclide in the sample, a completely

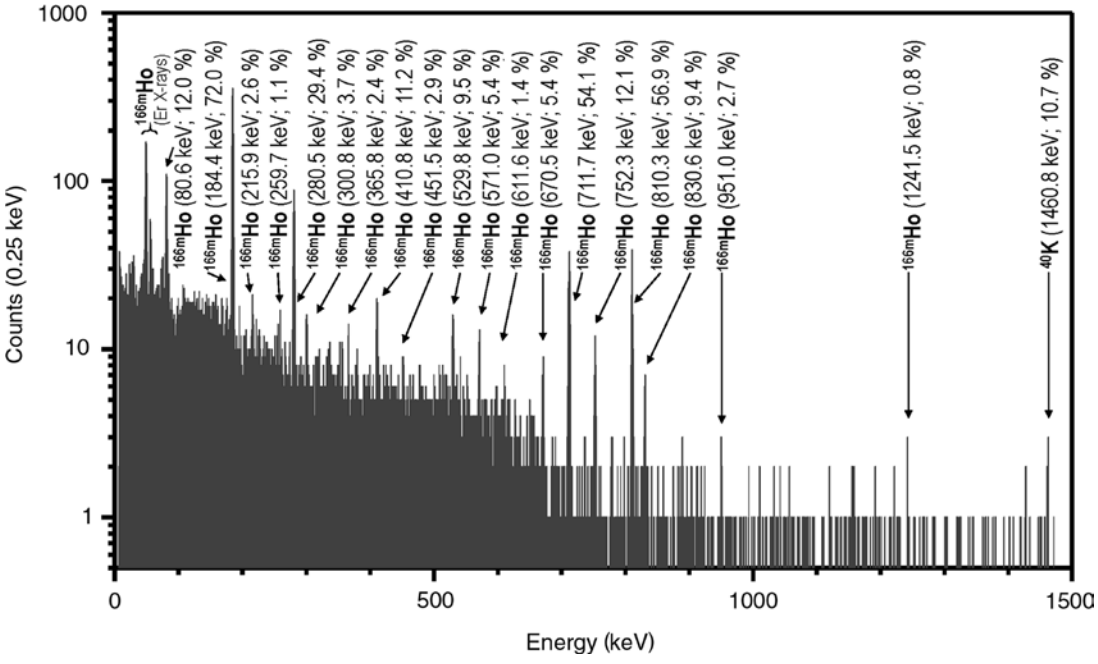

Figure 3: Spectrum from γ-ray spectrometry (real counting time 603 s) of the residue from the evaporation of the unified Ho-containing fractions which were obtained by processing of the 30 mg Er target.

flat γ-ray spectrum without any peaks above background would result. The obtained γ-ray spectrum of Ho isolated from the 30 mg Er target is shown in Figure 3.

All lines prominently visible in the spectrum originate from ^{166m}Ho, which passed the chemical separation procedure along with ^{163}Ho. Quantitative analysis revealed activities of (16.0 ± 1.3) Bq ^{166m}Ho (Ho from the 6.7 mg target) and (7.0 ± 0.4) kBq ^{166m}Ho (Ho from the 30 mg target). No evidence for the presence of ^{170}Tm was found; from the absence of counts above background at the energy of 84 keV (i.e., the position of the main peak of ^{170}Tm), an activity of ^{170}Tm of <7 kBq follows.

The contents of species in the mass range of 157–174 u (i.e. including ^{163}Ho) were quantified with ICP-MS. The content of Ho was calibrated for stable ^{165}Ho. The content of ^{165}Ho in the whole Ho preparations was determined to $(4.53 \pm 0.07) \cdot 10^{15}$ atoms (Ho from 6.7 mg target) and $(6.29 \pm 0.78) \cdot 10^{17}$ atoms (Ho from 30 mg target).

In a next step, the isobar ratios were determined. The results given as percentage in Table 3.

All nuclides, which are stable or have sufficiently long half-lives to still be present in the Ho preparations at the time of the ICP-MS measurement (performed ~980 days after the chemical separation), are therefore given in the second column of Table 3. The observed isobar ratios show that in the mass region 157–174 u (lanthanides from Gd to Lu) the mass 163 u is clearly the major constituent in both samples. Since this method cannot resolve the very minor mass difference between isobars, only information about the sum of all isobars of a certain mass number, but no information on the contribution of isobars from different elements is obtained.

The Ho-fraction isolated from the 6.7 mg Er target contains almost exclusively species of mass 163 u (about 89 %) and mass 165 u (about 11 %). The latter mass is entirely ascribed to ^{165}Ho, as this is the only stable or long-lived mass 165 u isobar. The signals from the neighboring masses 162 u and 164 u accounting for less than 0.2 % of the total mass might originate from Dy impurities or might be due to a neighbor-mass effect of the huge mass 163 u signal. An origin due to ^{162}Er and ^{164}Er from the target, which might have remained in the Ho after the chemical isolation, is ruled out, since ^{166}Er and ^{168}Er were more abundant in the Er target used, but are not present. The results of all other examined masses are below the range of uncertainty or equal to or below the background measurement.

In the Ho sample isolated from the 30 mg target, the most abundant isobars are again at mass 163 u (^{163}Dy and ^{163}Ho) with about 57 %, followed by the one at 165 u with nearly 30 %, which is ^{165}Ho. Additionally, the masses 162 u, 164 u, 166 u, 168 u, and 170 u contribute between about 0.8 % and 5 % for each isobar (cf. Table 3). These are attributed to the stable Er-isotopes from the irradiation target, which have remained in the Ho fraction. To confirm this, the isotopic composition of the Er obtained from the post-irradiation chemical separation was determined in separate ICP-MS measurements. The results agree well with those of the isotopic composition of Er in the Ho fraction, cf. Table 4.

^{167}Er is missing, because it has been extensively burned up during the long irradiation duration due to its high thermal neutron capture cross section of ca. 650 barn [23]. The relative content at 164 u with respect to the other masses due to Er isotopes is higher in the Ho fraction than in the separate analysis of the Er fraction. This is due to the presence of some ^{164}Dy, which was formed in the neutron

Table 3: Results of the ICP-MS measurements of the examined isobars, given as percentages of the samples.

Mass (u)	Nuclide(s)	Ho fraction of the 6.7 mg target (%)	Ho fraction of the 30 mg target (%)
157	^{157}Gd	–[a]	0.05 ± 0.39
158	^{158}Gd, ^{158}Dy	–[a]	–[a]
159	^{159}Tb	–[a]	–[a]
160	^{160}Gd, ^{160}Dy	0.01 ± 0.04	0.11 ± 0.33
161	^{161}Dy	0.03 ± 0.05	–[a]
162	^{162}Dy, ^{162}Er	0.11 ± 0.06	2.17 ± 0.86
163	^{163}Dy, ^{163}Ho	88.62 ± 0.50	57.45 ± 2.53
164	^{164}Dy, ^{164}Er	0.07 ± 0.06	1.06 ± 0.68
165	^{165}Ho	11.10 ± 0.46	29.17 ± 0.91
166	^{166m}Ho, ^{166}Er	0.02 ± 0.04	3.72 ± 0.56
167	^{167}Er	–[a]	0.31 ± 0.33
168	^{168}Er, ^{168}Yb	0.01 ± 0.03	4.89 ± 0.97
169	^{169}Tm	0.01 ± 0.02	–[a]
170	^{170}Er, ^{170}Tm, ^{170}Yb	–[a]	0.83 ± 0.59
171	^{171}Tm, ^{171}Yb	–[a]	0.16 ± 0.20
172	^{172}Yb	–[a]	0.06 ± 0.29
173	^{173}Yb	0.01 ± 0.02	0.02 ± 0.29
174	^{174}Yb, ^{174}Hf	0.01 ± 0.03	–[a]

[a]Value below or equal to background.

Table 4: Results of the ICP-MS measurements of the isobars that contain a stable Er-isotope.

Mass (u)	Nuclide(s)	Ho fraction of the 30 mg target (%)	Er fraction of the 30 mg target (%)
162	^{162}Dy, ^{162}Er	17.1	17
164	^{164}Dy, ^{164}Er	8.4	4
166	^{166m}Ho, ^{166}Er	29.4	31
167	^{167}Er	–	2
168	^{168}Er, ^{168}Yb	38.6	39
170	^{170}Er, ^{170}Tm, ^{170}Yb	6.5	7

The values are normalized to the sum of all these isobars equaling 100 %.

capture of the product nuclide ^{163}Ho, as was confirmed in the later stages of the analysis (cf. Table 7). For all other analyzed masses, the findings do not exceed the levels of the background measurement or are lower than the range of uncertainty of the measurements.

Combination of the quantitative results for ^{165}Ho and the isobaric ratios given in Table 3 lead to the absolute atom numbers of the contribution on mass 163 u (^{163}Dy and ^{163}Ho). These were determined to $(3.62 \pm 0.16) \cdot 10^{16}$ atoms on mass 163 u (Ho fraction from the 6.7 mg target) and $(1.24 \pm 0.17) \cdot 10^{18}$ atoms of mass 163 u (Ho fraction from the 30 mg target).

The ICP-MS technique does not allow to differentiate between the desired product nuclide ^{163}Ho and impurities of ^{163}Dy. To this end, RIMS was additionally applied, which combines elemental-specific ionization induced by resonant multi-step laser excitation with magnetic mass separation. It is thus an excellent method to obtain precise isotope ratios of a given chemical element. For these measurements, which were carried out at the RISIKO mass separator, avoiding (or at least minimizing) surface ionization on hot parts of the ion source, was key, as this kind of ionization is not element specific among the rare earth metals. This condition was ensured by keeping the ion source temperature low enough to prevent significant contributions from surface ionization, but high enough to facilitate thermal decomposition of the lanthanide nitrate (hydrate) to the lanthanide oxide, followed by reduction of the lanthanide oxide to the metal, and finally sublimation of at least parts of the solid lanthanide metal under the high vacuum conditions. This yielded a stable ion beam formed almost exclusively by resonant laser ionization. A sputtered Y layer served as an agent for the reduction of the lanthanide oxide at the comparatively low temperatures. Information on the contribution from surface ionization was obtained by monitoring the 165 u mass signal. As there is no stable Dy-isotope on this isobar, but sufficient amounts of ^{165}Ho (see Table 3) for unspecific surface ionization in both samples, the appearance (and magnitude) of a 165 u signal in the mass scan would be precisely indicating any contribution from surface ionization. However, this was found to be of negligible influence on the results of the Dy isotopic distribution in both Ho samples.

Table 5: Isotopic distribution (in %) of the Dy content in the Ho samples obtained via RIMS.

Dy-isotope	Natural abundance	Ho fraction of the 6.7 mg target (%)	Ho fraction of the 30 mg target (%)
^{160}Dy	2.329	1.6 ± 0.1	0.5 ± 0.2
^{161}Dy	18.889	13.5 ± 0.6	4.2 ± 0.8
^{162}Dy	25.475	29.9 ± 0.5	8.0 ± 0.8
^{163}Dy	24.896	29.9 ± 0.3	14.1 ± 0.6
^{164}Dy	28.260	25.1 ± 0.9	73.5 ± 2.2

These numbers show different distributions of the stable Dy isotopes in both analyzed aliquots, which also significantly differ from the abundances in natural Dy (cf. Table 5). While perhaps surprising at first glance, this can be understood by considering the different history of these Dy-isotopes.

First, some Dy of unknown isotopic distribution remained in the Er targets after the prepurification (see Section 3.1) and might have ended up in the Ho fraction. Since the material underwent isotopic enrichment (aimed at ^{162}Er), the isotopic composition also of the Dy impurities might differ from the natural abundance. Secondly, during the irradiation the isotopic ratios were changed as isotopes having a comparatively high neutron capture cross section like ^{164}Dy (2650 b) and ^{161}Dy (600 b) were burned up to a larger extent than others with lower cross sections. The content of the latter ones might rather have increased due to formation through neutron capture of the neighboring lighter isotope. At all steps of handling described above there always was the possibility of having introduced some impurities of Dy of natural isotopic composition. If this had happened before irradiation the isotopic distribution was changed, otherwise not. For verification of the absence of any input of Dy through the materials applied for the RIMS measurement (i.e. the Zr foil and the sputtered metallic Y) background measurements with blanks of these materials were performed. Obtaining stable beams of Dy-ions with enough intensity for measurement was impossible from these samples. Therefore, the Zr foil and the sputtered Y layer can be excluded as further significant source of Dy in the RIMS measurement. Additionally, ^{163}Dy was continuously produced from the decay of ^{163}Ho (about 0.04 % of the initially obtained ^{163}Ho were thus converted into ^{163}Dy during the 980 days period) and ^{164}Dy had been formed during the irradiation from the product burn up of ^{163}Ho through neutron capture to ^{164}Ho ($T_{1/2} = 29$ min, 40 % β^- decay, 60 % EC decay) and the following EC decay.

Based on these facts, the isotope content of Dy in the Ho fraction isolated from the 6.7 mg Er target can be supposed to be mainly due to an impurity, which was already present in the Er target. The initial Dy isotopic distribution underwent some changes during irradiation. Addition of ^{163}Dy and ^{164}Dy occurred through the above described processes of the decay and burn up of product nuclide ^{163}Ho. In contrast to this, Dy in the Ho fraction isolated from the 30 mg Er target was predominantly consisting of the isotope ^{164}Dy and only to a much lower extent of ^{163}Dy, whereas the other Dy isotopes were only present in minor

shares. Therefore, Dy was mostly originating from burn up of ^{163}Ho and at much lower level from decay of already produced ^{163}Ho. Impurities of Dy in the target or introduced during the processing procedure played only a marginal role as Dy sources in this sample.

Thanks to the RIMS results, the Dy isotope ratios were now known, though not yet their absolute amounts. This, however, is needed for the 163 u isobar differentiation between ^{163}Ho and ^{163}Dy. To get information on the absolute atom numbers of all examined Dy isotopes, it was sufficient to determine this for one Dy isotope. The values of the other isotopes can be calculated from the obtained isotope ratios. Neutron activation analysis (NAA) offers the possibility to easily specify the absolute atom number of ^{164}Dy. This nuclide undergoes thermal neutron capture with high cross section to ^{165}Dy ($T_{1/2} = 2.33$ h), which can then be measured by γ-ray spectrometry. Additionally it gives also results for other potentially existent elements if they are accessible by this analytical method.

For correct quantification of the particular isotopes knowledge of the thermal neutron flux during the activation is indispensable. Therefore standard samples of known amounts of gold were co-irradiated and afterwards analyzed by γ-ray spectrometry. Neutron flux values of $(8.48 \pm 0.17) \cdot 10^{11}$ cm$^{-2} \cdot$ s^{-1} at the bottom and $(8.59 \pm 0.15) \cdot 10^{11}$ cm$^{-2} \cdot$ s^{-1} at the top of the stacked samples were evaluated. The thermal neutron flux which the samples were exposed to is assumed to be the average, as the samples were located between the irradiation positions of the gold standards, i.e. $(8.54 \pm 0.11) \cdot 10^{11}$ cm$^{-2} \cdot$ s^{-1}. This value has been used for further evaluation of the NAA results.

The γ-ray spectra of irradiated aliquots of the Ho samples showed the activation products ^{24}Na, ^{165}Dy, ^{166}Ho, ^{167}Ho, and ^{171}Er (besides ^{166m}Ho, which was present already in the original samples). From these, the contents of stable (or long lived) impurities of ^{23}Na, ^{164}Dy, ^{165}Ho, ^{166m}Ho, and ^{170}Er as given in Table 6 were evaluated.

The results show a rather large amount of stable sodium to be present in the samples. This is probably a contamination from the glass container, in which the solution has been stored since its production. It will, however, be quantitatively eliminated in the subsequent mass separation step and is hence of no concern. The content of ^{164}Dy is more than a factor of 100 smaller than the ^{165}Ho content or the sum of the 163 u isobar. The ^{165}Ho contents determined via NAA are about 15 % (Ho from 6.7 mg Er target) and about 25 % (Ho from 30 mg Er target) higher than those determined via ICP-MS. This could be due to an epithermal neutron component present in the neutron spectrum used in the NAA leading to more efficient activation of ^{165}Ho compared to that of ^{197}Au, due to differences in epithermal to thermal activation cross section ratios for the two reactions. The neutron capture cross section value of ^{165}Ho and ^{197}Au used for the calculations are for a purely thermal neutron spectrum. Due to the high thermal neutron capture cross section of ^{166m}Ho of 3100 barn and therefore the high sensitivity of NAA, the long-lived radionuclide ^{166m}Ho, contained in comparatively small amounts, was also found via the detection of ^{167}Ho in both of the aliquots. The contents of ^{166m}Ho as determined via NAA are in good agreement with those obtained via γ-ray spectrometry (see above at the beginning of this section). Remains of the Er target due to incomplete separation which are visible via the activation of ^{170}Er in NAA, were only located in the Ho fraction from the 30 mg target, whereas no evidence of Er was measured in Ho from the 6.7 mg Er target. Further, no hints for the presence of stable or long-lived Tm isotopes in either sample were seen.

In addition to the mentioned nuclides ^{24}Na, ^{165}Dy, ^{166}Ho, ^{167}Ho, and ^{171}Er, activities of (46.8 ± 6.3) kBq ^{164m}Ho ($T_{1/2} = 37$ min) and (390 ± 15) kBq ^{164g}Ho ($T_{1/2} = 29$ min) were formed during the neutron activation in the aliquot of Ho from the 6.7 mg Er target as well as (17.0 ± 2.4) kBq ^{164m}Ho and (138.3 ± 5.2) kBq ^{164g}Ho in the aliquot of Ho from the 30 mg Er target. The production of both isomers of ^{164}Ho can be described by eq. (2)–(4):

$$A_{^{164m}\mathrm{Ho}} = N_{^{163}\mathrm{Ho}} \cdot \sigma_{^{163}\mathrm{Ho}\rightarrow{}^{164m}\mathrm{Ho}} \cdot \phi \cdot \left(1 - e^{-\lambda_{^{164m}\mathrm{Ho}} \cdot t_I}\right) \tag{2}$$

$$A_{^{164g}\mathrm{Ho}}(\text{direct activation}) = N_{^{163}\mathrm{Ho}} \cdot \sigma_{^{163}\mathrm{Ho}\rightarrow{}^{164g}\mathrm{Ho}} \cdot \phi \cdot \left(1 - e^{-\lambda_{^{164g}\mathrm{Ho}} \cdot t_I}\right) \tag{3}$$

$$A_{^{164g}\mathrm{Ho}}(\text{indirect activation}) = N_{^{163}\mathrm{Ho}} \cdot \sigma_{^{163}\mathrm{Ho}\rightarrow{}^{164m}\mathrm{Ho}} \cdot \phi \cdot \left(1 + \frac{\lambda_{^{164g}\mathrm{Ho}} \cdot e^{-\lambda_{^{164m}\mathrm{Ho}} \cdot t_I} - \lambda_{^{164m}\mathrm{Ho}} \cdot e^{-\lambda_{^{164g}\mathrm{Ho}} \cdot t_I}}{\lambda_{^{164m}\mathrm{Ho}} - \lambda_{^{164g}\mathrm{Ho}}}\right) \tag{4}$$

where $N_{^{163}\mathrm{Ho}}$ is the number of ^{163}Ho atoms, ϕ the thermal neutron flux, λ_i the decay constant of isotope i, and t_I the duration of the neutron activation. $\sigma_{^{163}\mathrm{Ho}\rightarrow{}^{164m}\mathrm{Ho}}$ is the

Table 6: Number of atoms of detected nuclides in the whole samples as resulted from the NAA.

Nuclide	Ho fraction of the 6.7 mg target (atoms)	Ho fraction of the 30 mg target (atoms)
^{23}Na	$(1.1 \pm 0.1) \cdot 10^{18}$	$(3.5 \pm 0.2) \cdot 10^{18}$
^{164}Dy	$(2.5 \pm 0.2) \cdot 10^{13}$	$(6.3 \pm 0.3) \cdot 10^{15}$
^{165}Ho	$(5.3 \pm 0.2) \cdot 10^{15}$	$(7.7 \pm 0.3) \cdot 10^{17}$
^{166m}Ho	$(1.4 \pm 0.3) \cdot 10^{12}$	$(3.5 \pm 0.2) \cdot 10^{14}$
^{170}Er	–	$(1.5 \pm 0.3) \cdot 10^{16}$

thermal neutron capture cross section of ^{163}Ho to ^{164m}Ho, and $\sigma_{^{163}\mathrm{Ho}\rightarrow{}^{164g}\mathrm{Ho}}$ the thermal neutron capture cross section of ^{163}Ho to ^{164g}Ho.

Equation (2) gives the activity of ^{164m}Ho at the end of bombardment (EOB), which has been formed by neutron capture of ^{163}Ho with thermal neutron capture cross section $\sigma_{^{163}\mathrm{Ho}\rightarrow{}^{164m}\mathrm{Ho}}$. Analogous to this, eq. (3) leads to the activity of ^{164g}Ho at EOB, which has been directly produced from ^{163}Ho with the thermal neutron capture cross section $\sigma_{^{163}\mathrm{Ho}\rightarrow{}^{164g}\mathrm{Ho}}$. In eq. (4) ^{164g}Ho has been formed as the metastable state isomer ^{164m}Ho (with thermal neutron capture cross section $\sigma_{^{163}\mathrm{Ho}\rightarrow{}^{164m}\mathrm{Ho}}$), but already decayed to ^{164g}Ho during the neutron activation. The total activity of ^{164g}Ho at EOB is thus the sum of eq. (3) and (4). Equations (2)–(4) do neither consider the target burn-up of ^{163}Ho during the neutron irradiation, which is insignificant (less than 1 % deviation up to $\sigma_{^{163}\mathrm{Ho}\rightarrow{}^{164m}\mathrm{Ho}}+\sigma_{^{163}\mathrm{Ho}\rightarrow{}^{164g}\mathrm{Ho}}=\sigma_{^{163}\mathrm{Ho}}>3\cdot10^{6}$ b under the applied irradiation conditions), nor the negligible decay of ^{163}Ho in the time frame of activation, cooling, and measurement due to the comparatively very long half-life. Also, neutron capture of $^{164m+g}$Ho, which is insignificant under these conditions, is neglected.

Since thermal neutron capture cross sections of ^{163}Ho to both states in ^{164}Ho, $\sigma_{^{163}\mathrm{Ho}\rightarrow{}^{164m}\mathrm{Ho}}$ and $\sigma_{^{163}\mathrm{Ho}\rightarrow{}^{164g}\mathrm{Ho}}$ are unknown, but the activities of ^{164m}Ho and ^{164g}Ho were experimentally determined in our experiments, it is possible to obtain the values for $\sigma_{^{163}\mathrm{Ho}\rightarrow{}^{164m}\mathrm{Ho}}$ and $\sigma_{^{163}\mathrm{Ho}\rightarrow{}^{164g}\mathrm{Ho}}$. Inserting of the data and solving these equations lead to $\sigma_{^{163}\mathrm{Ho}\rightarrow{}^{164m}\mathrm{Ho}}=(22.6\pm3.2)$ b and $\sigma_{^{163}\mathrm{Ho}\rightarrow{}^{164g}\mathrm{Ho}}=(155.0\pm10.0)$ b for ^{163}Ho from the 6.7 mg Er target as well as $\sigma_{^{163}\mathrm{Ho}\rightarrow{}^{164m}\mathrm{Ho}}=(24.2\pm4.8)$ b and $\sigma_{^{163}\mathrm{Ho}\rightarrow{}^{164g}\mathrm{Ho}}=(160.1\pm24.6)$ b for ^{163}Ho from the 30 mg Er target. From these values the thermal neutron capture cross section of ^{163}Ho was evaluated to $\sigma_{^{163}\mathrm{Ho}\rightarrow{}^{164m}\mathrm{Ho}}=(23\pm3)$ b and $\sigma_{^{163}\mathrm{Ho}\rightarrow{}^{164g}\mathrm{Ho}}=(156\pm9)$ b for the formation of the two isomers of ^{164}Ho.

Applying the values of $\sigma_{^{163}\mathrm{Ho}\rightarrow{}^{164m}\mathrm{Ho}}=23$ b and $\sigma_{^{163}\mathrm{Ho}\rightarrow{}^{164g}\mathrm{Ho}}=156$ b as cross sections for the product burn-up in eq. (1), the irradiation yield for ^{163}Ho that was estimated in Section 3.1 (cf. Table 2) reduces from $4.4\cdot10^{16}$ atoms ^{163}Ho to $4.2\cdot10^{16}$ atoms ^{163}Ho for the 6.7 mg Er-target and from $2.4\cdot10^{18}$ atoms ^{163}Ho to $1.4\cdot10^{18}$ atoms ^{163}Ho for the 30 mg Er target. These data are closer to the experimentally obtained yields of $(3.64\pm0.16)\cdot10^{16}$ atoms ^{163}Ho (6.7 mg Er target) and $(1.30\pm0.18)\cdot10^{18}$ atoms ^{163}Ho (30 mg Er target). The residual discrepancies are easily accounted for by the difference of perturbed and unperturbed neutron flux.

Combining the data obtained from the different analytical methods allows for a comprehensive characterization of both Ho-samples. These final results are given in Table 7.

Table 7: Number of atoms in the total Ho samples obtained from the combination of the results from all analytical techniques.

Nuclide	(atoms)	Share[a] (%)	Analytical technique(s)
	Ho fraction of the 6.7 mg target		
^{23}Na	$(1.1\pm0.1)\cdot10^{18}$	–	NAA
^{160}Dy	$(1.6\pm0.2)\cdot10^{12}$	0.004	RIMS, NAA
^{161}Dy	$(1.3\pm0.2)\cdot10^{13}$	0.032	RIMS, NAA
^{162}Dy	$(3.0\pm0.3)\cdot10^{13}$	0.074	RIMS, NAA
^{163}Dy	$(3.0\pm0.3)\cdot10^{13}$	0.074	RIMS, NAA
^{164}Dy	$(2.5\pm0.2)\cdot10^{13}$	0.062	NAA
^{163}Ho	$(3.6\pm0.2)\cdot10^{16}$	89.000	ICP-MS, RIMS, NAA
^{165}Ho	$(4.5\pm0.1)\cdot10^{15}$	11.000	ICP-MS
^{166m}Ho	$(8.7\pm0.7)\cdot10^{11}$	0.002	γ-ray spectrometry
	Ho fraction of the 30 mg target		
^{23}Na	$(3.5\pm0.2)\cdot10^{18}$	–	NAA
^{160}Dy	$(4.3\pm1.8)\cdot10^{13}$	0.002	RIMS, NAA
^{161}Dy	$(3.6\pm0.8)\cdot10^{14}$	0.018	RIMS, NAA
^{162}Dy	$(6.9\pm0.8)\cdot10^{14}$	0.034	RIMS, NAA
^{163}Dy	$(1.2\pm0.1)\cdot10^{15}$	0.059	RIMS, NAA
^{164}Dy	$(6.3\pm0.3)\cdot10^{15}$	0.310	NAA
^{163}Ho	$(1.2\pm0.2)\cdot10^{18}$	59.000	ICP-MS, RIMS, NAA
^{165}Ho	$(6.3\pm0.8)\cdot10^{17}$	31.000	ICP-MS
^{166m}Ho	$(3.8\pm0.3)\cdot10^{14}$	0.019	γ-ray spectrometry
^{162}Er	$(3.4\pm0.7)\cdot10^{16}$	1.700	NAA, ICP-MS
^{164}Er	$(8.7\pm1.7)\cdot10^{15}$	0.430	NAA, ICP-MS
^{166}Er	$(6.2\pm1.2)\cdot10^{16}$	3.000	NAA, ICP-MS
^{167}Er	$(4.2\pm0.8)\cdot10^{15}$	0.210	NAA, ICP-MS
^{168}Er	$(7.5\pm1.5)\cdot10^{16}$	3.700	NAA, ICP-MS
^{170}Er	$(1.5\pm0.3)\cdot10^{16}$	0.740	NAA

[a]Normalized to the total content in the mass region around A = 163, i.e. without considering ^{23}Na, which is easily quantitatively removed in the mass separation step.

The desired product nuclide ^{163}Ho is the main component in both samples, with the exception of large amounts of stable sodium. The isobaric Dy-isotope ^{163}Dy contributes a share of only (0.08 ± 0.01) % (Ho from the 6.7 mg Er target) and (0.10 ± 0.02) % (Ho from the 30 mg Er target) to the 163 u isobar and is thus insignificant in both samples.

3.4 Magnetic isotope separation for isolation of ^{163}Ho from chemically purified Ho fractions

As follows from Table 7, the atom ratios of ^{166m}Ho:^{163}Ho varies for individual samples, and reaches a value of $<4\cdot10^{-4}$ in the sample with the higher concentration. To comply with the requirements of maximum concentrations of $5\cdot10^{-8}$ in the current phase and $5\cdot10^{-9}$ in the next phase of the ECHo project (cf. Section 8.4 in [1]), further suppression by an additional factor of at least $3\cdot10^{-5}$ is thus necessary. This was achieved by applying magnetic isotope separation at

RISIKO and at the GPS/CERN-ISOLDE. Using the prepared samples of stable Ho, the ionization- and transmission-efficiency of the resonant laser ionization at the RISIKO mass separator has been determined to be (32 ± 5) % for Ho [14]. First implantations of ^{163}Ho into ECHo MMC detectors have been performed at RISIKO [1].

By utilizing a sample of $1.2 \cdot 10^{14}$ atoms ^{163}Ho a separation run was performed at the GPS of ISOLDE, which resulted in implantation of about $4 \cdot 10^{10}$ atoms ^{163}Ho into each of the 32 MMC pixels of one detector chip. It has been used for test measurements, obtained results are published in [3].

4 Conclusion

The strategy for the production of radiochemically pure ^{163}Ho samples has been described. This involves target pre-purification, neutron irradiation, as well as post irradiation target processing. Samples of $>10^{18}$ atoms of ^{163}Ho have been isolated, sufficient for the current stages of the ECHo project. By performing a similar production sequence, but starting with moderately larger samples of more highly enriched ^{162}Er, samples on the order of 10^{19} atoms can be obtained, as needed for the next phase of the ECHo project. The Ho samples obtained by chemical separation were characterized by various analytical methods, i.e. ICP-MS, RIMS, and NAA, which verified the suitability of the final samples for their use within the current and future stages of the ECHo-project. The only radioactive impurity that was identified in the chemically isolated Ho samples was ^{166m}Ho, present at levels of $<4 \cdot 10^{-4}$ with respect to ^{163}Ho (cf. Table 7). For its further suppression, magnetic mass separation is applied, providing an additional separation factor on the order of 10^{-5}, leading to samples of the purity as required for the ECHo project [1, 14]. This last separation step also serves for the ion-implantation of ^{163}Ho into the ECHo MMCs used for the neutrino mass determination within the ECHo-project.

Acknowledgements: This work was carried out in the framework of the DFG Research Unit FOR 2202 (ECHo) and we acknowledge financial support from the DFG under contracts DU 1334/1-1, EN 299/7-1, and GA 2219/2-1. H.D. acknowledges additional support by the Stufe 1 funding of the Johannes Gutenberg University Mainz. This project has received funding through the European Union's Seventh Framework Programme for Research and Technological Development under Grant Agreements 262010 (ENSAR), 267194 (COFUND), and 289191 (LA^{3}NET). The authors would like to thank Alexander Voegele for irradiating samples for the Ho and Er tracer at SINQ, Silvia Koechli and Anja Eichler for performing the ICP-OES measurements, Tobias Reich and Samer Amayri for performing the ICP-MS analytics as well as Ernst Schaub for technical assistance.

References

1. Gastaldo, L., Blaum, K., Chrysalidis, K., Goodacre, T. D., Domula, A., Door, M., Dorrer, H., Düllmann, Ch. E., Eberhardt, K., Eliseev, S., Enss, C., Faessler, A., Filianin, P., Fleischmann, A., Fonnesu, D., Gamer, L., Haas, R., Hassel, C., Hengstler, D., Jochum, J., Johnston, K., Kebschull, U., Kempf, S., Kieck, T., Köster, U., Lahiri, S., Maiti, M., Mantegazzini, F., Marsh, B., Neroutsos, P., Novikov, Yu.N., Ranitzsch, P. C. O., Rothe, S., Rischka, A., Saenz, A., Sander, O., Schneider, F., Scholl, S., Schüssler, R. X., Schweiger, Ch., Simkovic, F., Stora, T., Szücs, Z., Türler, A., Veinhard, M., Weber, M., Wegner, M., Wendt, K., Zuber, K.: The electron capture ^{163}Ho experiment – ECHo. Eur. Phys. J. Spec. Top. **226**, 1623 (2017).
2. Gastaldo, L., Blaum, K., Doerr, A., Düllmann, Ch. E., Eberhardt, K., Eliseev, S., Enss, C., Faessler, A., Fleischmann, A., Kempf, S., Krivoruchenko, M., Lahiri, S., Maiti, M., Novikov, Yu. N., Ranitzsch, P. C.-O., Simkovic, F., Szusc, Z., Wegner, M.: The electron capture ^{163}Ho experiment ECHo. J. Low Temp. Phys. **176**, 876 (2014).
3. Hassel, C., Blaum, K., Goodacre, T. D., Dorrer, H., Düllmann, Ch. E., Eberhardt, K., Eliseev, S., Enss, C., Filianin, P., Fäßler, A., Fleischmann, A., Gastaldo, L., Goncharov, M., Hengstler, D., Jochum, J., Johnston, K., Keller, M., Kempf, S., Kieck, T., Köster, U., Krantz, M., Marsh, B., Mokry, C., Novikov, Yu. N., Ranitzsch, P. C. O., Rothe, S., Rischka, A., Runke, J., Saenz, A., Schneider, F., Scholl, S., Schüssler, R. X., Simkovic, F., Stora, T., Thörle-Pospiech, P., Türler, A., Veinhard, M., Wegner, M., Wendt, K., Zuber, K.: Recent results for the ECHo experiment. J. Low Temp. Phys. **184**, 910 (2016).
4. Baisden, P. A., Sisson, D. H., Niemeyer, S., Hudson, B., Bennett, C. L., Naumann, R. A.: Measurement of the half-life of ^{163}Ho. Phys. Rev. C **28**, 337 (1983).
5. Gastaldo, L.: In: E. Kearns, G. Feldman (Eds.), XXVI Int. Conf. Neutrino Physics and Astrophysics: Neutrino 2014 (2015), AIP Publishing LLC, Boston, MA, USA, Vol. 1666, p. 050001.
6. Faler, K. T.: Determination of the half-life of the longer-lived ^{166}Ho isomer. J. Inorg. Nucl. Chem. **27**, 25 (1965).
7. Engle, J. W., Birnbaum, E. R., Trellue, H. R., John, K. D., Rabin, M. W., Nortier, F. M.: Evaluation of ^{163}Ho production options for neutrino mass measurements with microcalorimeter detectors. Nucl. Instrum. Methods B **311**, 131 (2013).
8. Maiti, M., Lahiri, S., Szücs, Z.: Separation of ^{163}Er from dysprosium target: a step toward neutrino mass measurement through electron capture of ^{163}Ho. J. Radioanal. Nucl. Chem. **307**, 1667 (2016).
9. Mocko, V., Taylor, W. A., Nortier, F. M., Engle, J. W., Barnhart, T. E., Nickles, R. J., Pollington, A. D., Kunde, G. J., Rabin, M. W., Birnbaum, E. R.: Isolation of ^{163}Ho from dysprosium target material by HPLC for neutrino mass measurements. Radiochim. Acta **103**, 577 (2015).

10. Guéguen, F., Isnard, H., Kossert, K., Bresson, C., Caussignac, C., Stadelmann, G., Nonell, A., Mialle, S., Chartier, F.: Purification of a ^{166m}Ho solution by successive high-performance liquid chromatography and gravitational chromatography for half-life determination. J. Radioanal. Nucl. Chem. **302**, 289 (2014).
11. Dadachova, E., Mirzadeh, S., Lambrecht, R. M., Hetherington, E. L., Knapp, F. F. Jr.: Separation of carrier-free holmium-166 from neutron-irradiated dysprosium targets. Anal. Chem. **66**, 4272 (1994).
12. Lahiri, S., Volkers, K. J., Wierczinski, B.: Production of ^{166}Ho through ^{164}Dy(n,γ) ^{165}Dy(n, γ) ^{166}Dy(β^-) ^{166}Ho and separation of ^{166}Ho. Appl. Radiat. Isot. **61**, 1157 (2004).
13. Gastaldo, L., Ranitzsch, P. C.-O., Seggern, F. v., Porst, J.-P., Schäfer, S., Pies, C., Kempf, S., Wolf, T., Fleischmann, A., Enss, C., Herlert, A., Johnston, K.: Characterization of low temperature metallic magnetic calorimeters having gold absorbers with implanted ^{163}Ho ions. Nucl. Instrum. Methods A **711**, 150 (2013).
14. Schneider, F., Chrysalidis, K., Dorrer, H., Düllmann, Ch. E., Eberhardt, K., Haas, R., Kieck, T., Mokry, C., Naubereit, P., Schmidt, S., Wendt, K.: Resonance ionization of holmium for ion implantation in microcalorimeters. Nucl. Instrum. Methods B **376**, 388 (2016).
15. Schneider, F., Beyer, T., Blaum, K., Block, M., Chenmarev, S., Dorrer, H., Düllmann, Ch. E., Eberhardt, K., Eibach, M., Eliseev, S., Grund, J., Köster, U., Nagy, Sz., Novikov, Yu. N., Renisch, D., Türler, A., Wendt, K.: Preparatory studies for a high-precision Penning-trap measurement of the ^{163}Ho electron capture Q-value. Eur. Phys. J. A **51**, 89 (2015).
16. Eliseev, S., Blaum, K., Block, M., Chenmarev, S., Dorrer, H., Düllmann, Ch. E., Enss, C., Filianin, P. E., Gastaldo, L., Goncharov, M., Köster, U., Lautenschläger, F., Novikov, Yu. N., Rischka, A., Schüssler, R. X., Schweikhard, L., Türler, A.: Direct measurement of the mass difference of ^{163}Ho and ^{163}Dy solves the Q-value puzzle for the neutrino mass determination. Phys. Rev. Lett. **115**, 062501 (2015).
17. Zimmer, K.: Bestimmung von ^{89}Sr und ^{90}Sr mit Resonanz-Ionisations-Spektroskopie in kollinearer Geometrie, PhD Thesis, Johannes Gutenberg University Mainz (1995).
18. Studer, D., Dyrauf, P., Naubereit, P., Heinke, R., Wendt, K.: Resonance ionization spectroscopy in dysprosium. Hyperfine Interact. **238**, 8 (2017).
19. Letokov, V. S.: Laser-induced processes in spectroscopy, isotope separation, and photochemistry. Sov. Phys. Usp. **29**, 70 (1986).
20. Kugler, E.: The ISOLDE facility. Hyperfine Interact. **129**, 23 (2000).
21. Mishin, V. I., Fedoseyev, V. N., Kluge, H.-J., Letokov, V. S., Ravn, H. L., Scheerer, F., Shirakabe, Y., Sundell, S., Tengblad, O. ISOLDE Collaboration: Chemically selective laser ion-source for the CERN-ISOLDE on-line mass separator facility. Nucl. Instrum. Methods B **73**, 550 (1993).
22. Rothe, S., Goodacre, T. D., Fedorov, D. V., Fedosseev, V. N., Marsh, B. A., Molkanov, P. L., Rossel, R. E., Seliverstov, M. D., Veinhard, M., Wendt, K. D. A.: Laser ion beam production at CERN-ISOLDE: new features – more possibilities. Nucl. Instrum. Methods B **376**, 91 (2016).
23. Danon, Y., Werner, C. J., Youk, G., Block, R. C., Slovacek, R. E., Francis, N. C.: Neutron total cross-section measurements and resonance parameter analysis of holmium, thulium, and erbium from 0.001 to 20 keV. Nucl. Sci. Eng. **128**, 61 (1998).